Minifluo and SeaExplorer glider Measurements from Statoil Troll field (Norway)

Mission report - NeXOS NOR-02 pre-demonstration

Fall 2016

Document prepared by Frédéric Cyr*

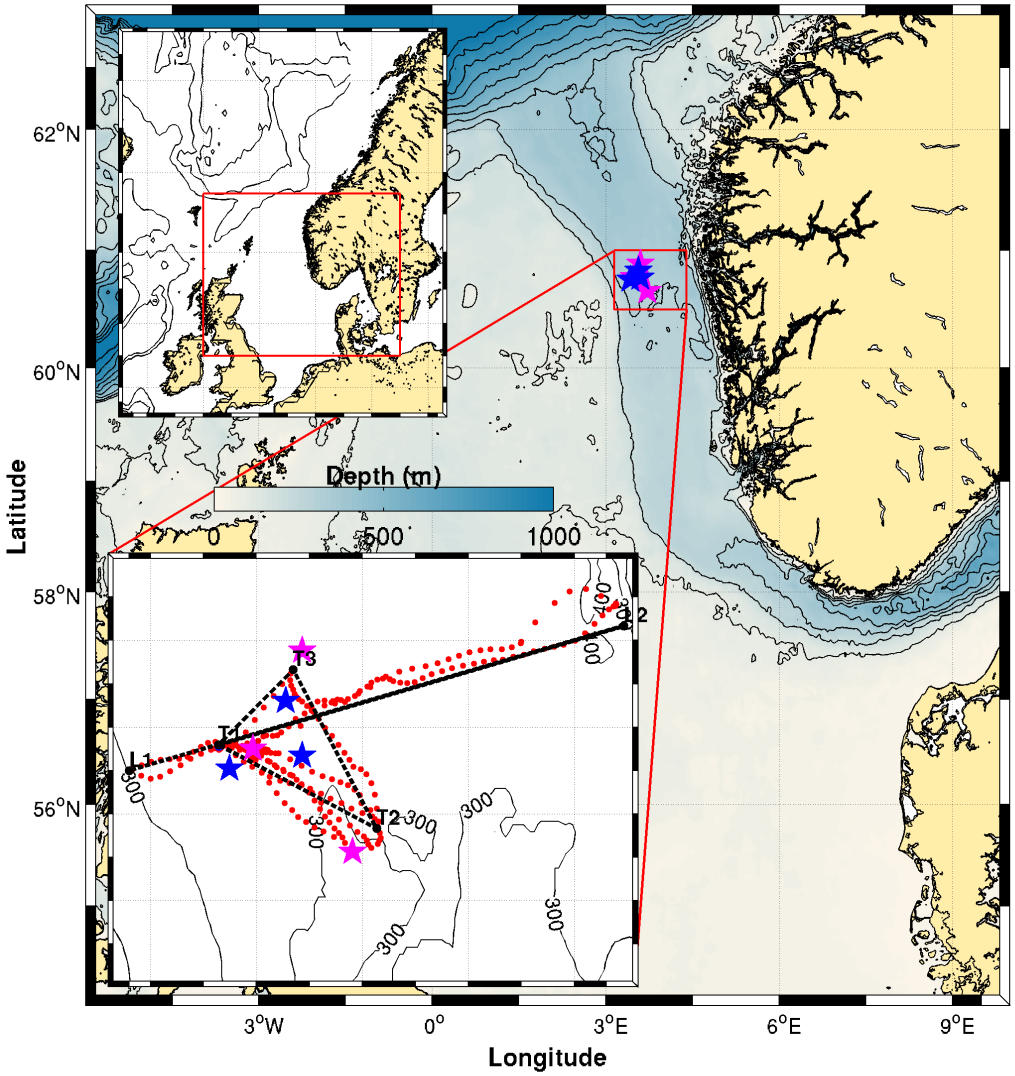

March 2017

*Frederic.Cyr@dfo-mpo.gc.ca

1 Context

This campaign was realized within the NeXOS [1]European project. As part of the Work Package 9 (*WP9 - Demonstrations of sensor systems performance*) leaded by the Runde Environment Centre in Norway, the target was to publicly demonstrate new sensor developments through real operational scenarios. It was realized as part of the task 9.2 (*Demonstrating optics and acoustics in North Atlantic waters on mobile and fixed platforms*). For this demonstration, partners Alseamar and Aix-Marseille University (AMU) have deployed the SeaExplorer glider SEA003 equipped with optical sensor O1 (Minifluo-UV) in proximity of oil & gas Troll field operated by Norwegian company Statoil. The deployment was realized between November 18$^{\text{th}}$ and December 3$^{\text{rd}}$, 2016. The present document reports preliminary results of this campaign.

To keep this report relatively short, some technical aspects are only discussed briefly, assuming that the reading is familiar with fluorescence measurements. Because this document will also be used to promote brainstorming between researchers participating the the mission, probably more figures than needed have been included. Many of these figures or panels are therefore not thoroughly discussed and can be ignored by the reader. The discussion is rather centered on the MiniFluo measurements and reference to specific figure panels are made within the text.

2 Summary of the campaign

Glider SeaExplorer SEA003 was deployed at waypoint $T1$ on 18 November 2016 (see map Figure 1). Water samples (4) were collected at deployment station (surface, 10 m, 25 m and 40 m) for further analysis in laboratory. The mission was completed according to the plan. First the glider completed a return transect across the channel along the $L1$-$L2$ line (roughly delimited by the isobath 300 m on both sides, see map Figure 1). Second, the glider completed a triangle delimited by waypoints $T1$-$T2$-$T3$-$T1$. Because these objectives were completed relatively quickly, it was decided to repeat the line $T1$-$T2$-$T1$ twice. Finally, while waiting for recovery, the glider stayed in virtual mooring mode (dives at the same geographical points) at proximity of Troll B. In the following, results from these different part of the deployment will be presented.

2.1 Logistics success of the campaign

Apart of the scientific aspects, the main goal of this campaign was to demonstrate the feasibility of using the MiniFluo/SeaExplorer package for an industrial offshore application. More precisely, the aim was to demonstrate that is it possible to 1) deploy and recover the SeaExplorer from a stand-by ship (Havila Troll) ; 2) maneuver the glider it this region subject to intense marine traffic ; 3) obtain and analyze meaningful data from the MiniFluo sensor (both in real- and delayed-mode time).

In the light of the results presented below, it is possible to say that these 3 objectives were fulfilled and that the demonstration was a success. The demonstration also shows that gliders equipped with relevant sensors are powerful environmental assessment tools that can be deployed with relative ease and with little scientific knowledge (e.g., we can easily imagine a deployment/recovery

1. Next generation Low-Cost Multifunctional Web Enabled Ocean Sensor Systems Empowering Marine, Maritime and Fisheries Management, is funded by the the European Commission's 7 Framework Programme - Grant Agreement No 614102

without scientists on board). As a matter of fact, the usual pre-deployment procedures at sea (radio communication with the glider and first dive with a floater attached) were skipped due to unfavorable weather conditions. The land pilot in France immediately took the control of the glider while communicating with the scientists at sea. For the recovery, no scientist were on board Havila Troll. Only few email exchanges with the Havila Troll bridge and a phone call the day of the recovery were sufficient. The glider was switched 'OFF', rinsed and put back in its transportation case by the Havila Troll crew. Glider SEA003 was brought on land during the subsequent crew change and was shipped back to France by Havila Troll transporter.

Only one important concern was reported by the Havila Troll crew regarding the recovery. For a reason still unknown, the antenna flasher was not working and, although the sea was very calm, the crew took about an hour to locate the glider. They finally spotted the glider with the searching light. The crew suggested to put reflective elements on the antenna (and possibly the wings) to help further recoveries with the searching light.

3 Scientific results and discussion

This section presents preliminary results of the campaign.

3.1 Comparison with *in situ* samples

Total Naphthalenes (Naps) and Phenanthrenes (Phes) concentrations (methylated and non-methylated) from the water samples collected at deployment site are given in Table 1. These were obtained by Gas Chromatography – Mass Spectrometry (GC-MS) analyses. Naphs concentrations exhibit smooth profile peaking in subsurface (10 m) before decreasing towards ∼40 m. Phes concentrations rather suggest a more erratic behavior, with a maximum at ∼25 m and two near-zero concentrations at 10 m and 40 m.

Comparison between these GC-MS measurements and the concentrations derived from in situ fluorescence measurements by the MiniFluo are presented in Figure 2. The solid black line represents the concentrations derived from laboratory calibrations on water accommodated fraction (WAF) of petroleum (procedure described in *Cyr et al.*, 2017). This procedure is used since oils/petroleum present in seawater contain a significant amount of methylated hydrocarbons (*Wang et al.*, 1999; *Guigue et al.*, 2011; *Adhikari et al.*, 2015), which are generally more fluorescent than the non-methylated parent hydrocarbons (*Ferretto et al.*, 2014). When possible, it is preferable to use the oil expected to be found on the field for the calibration (in order to have the good proportions of parent hydrocarbons). In the absence of oil samples from the Troll field, "Maya"-type crude oil originating from Mexico was used.

Discrepancies between fluorescence-derived concentrations and GC-MS measurements are specially important for Naphs, where the MiniFluo overestimated near-surface concentrations by more than a factor 5 (Figure 2, left panel). This overestimation is reduced when the raw data set is corrected for environmental blank value (see *Cyr et al.*, 2017, for discussion about this correction), that is when the minimum value of the relative-unit dataset is subtracted (dashed lines in Figure 2). In other words, when the minimum signal captured during the whole mission is assumed to be zero concentration.

Also, Naphs have the same excitation/emission wavelengths ($\lambda_{Ex}/\lambda_{Em}$: 275/340 nm) than the Tryptophan, an amino-acid naturally found in water and associated with microbial processes. In the absence of strong hydrocarbon signal (e.g., a significant spill), it is possible that part of the overestimation of Naphs by the MiniFluo is linked to a Tryptophan fluorescence signal. This might explain the overestimation observed in fluorescence-derived Naphs concentrations.

Surface Phes concentrations derived from the MiniFluo match surprisingly well those measured by GC-MS (Figure 2, right panel). The latter are however suspicious, specially the near-zero concentrations measured near 10 and 40 m. While the fluorescence profile is smooth, discrete GC-MS measurements are rather spiky. Nevertheless, it seems that the MiniFluo captures relatively well the bulk part of the Phes signal in the region. In order to get rid of uncertainties relative to the calibration procedure, relative-unit (RU) calibration will be used for the remainder of the report.

3.2 Surface concentrations

Surface concentration (in relative units) averaged over the top 10 m of the water column are shown in Figure 3. Highest concentrations are found along the first transect line across the channel, east/southeast of Songa Equinox (approximately 20 November). This higher concentration patch has disappeared during the return transect. Two other relatively high concentration patches were also detected, the first one at the channel edge near *Fensfjorden* entrance (between 21-22 November) and during the second passage near Troll A (29 November). At the very end of the mission, during the virtual mooring made at proximity of Troll B, the MiniFluo also captured higher than the average concentration for a period of about 24h (visible on the map only for Naphs channel).

Figure 3 suggests a relative spatio-temporal heterogeneity of this region. This is not surprising given the tidal dynamics and the winter winds at play during the survey. However, the coherence in successive glider profiles with the MiniFluo, shows the ability of the sensor to detect hydrocarbon path. When using laboratory calibration for Phe-like measurements (that are in relative agreement with the GC-MS measurements, Figure 2 right panel), the maximum surface concentration encountered during the mission is about 20 $\mathrm{ng\,L^{-1}}$ This is two orders of magnitude below the maximum admissible concentration of individual PAHs (2.4 $\mu\mathrm{g\,L^{-1}}$) set by the European Water Framework Directive (reported from *Nasher et al.*, 2013). Note that even if Naph-like concentration are likely overestimated by the laboratory calibration (Figure 2, left panel), values still remain below the maximum admissible concentration values at all times.

3.3 Across channel section

The two-way transect across the channel was projected along the $L1$-$L2$ line (Figures 4 and 5). As observed in Figure 3, patches of higher PAHs concentrations (Phe-like and Naph-like) are found during the first transect. This is specially clear in Phe-like fluorescence (Figure 4F) in the top $\sim$ 100 m of the water column and roughly between 20-40 km and 50-70 km. Interestingly, Phe-like signal is often contrasted with Chl-a signal, the former being maximum where the latter is minimum (specially clear in the 20-40 km range). Except very close to the surface, the Naph-like fluorescence (Figure 4E) is different from Phe-like signal (with notable electronic problems near 30, 50 and 60 km). While Phe-like patterns are reproduced in Naph-like signal, the latter seems to also reproduce some of the Chl-a patterns (« adding » panels D and F, which would

lead to a pattern close to the one in panel E). It is likely that the Naph-like channel also captures Tryptophan-like fluorescence that is associated with biological activities, and thus Chl-a. This is because Naphthalene $\lambda_{Ex}/\lambda_{Em}$ fluorescence couple is similar to the one of Tryptophan.

Also worth to note is the relatively high Phe-like fluorescence signal near the seafloor. This signal seems to reach surface concentration signal in Chimney-like patterns (not to be mistaken with vertical bars present in panel E that are likely resulting from problems with the sensor). These patterns are also reproduced in the CDOM (higher concentration, Figure 4G), in the O_2 (lower concentrations, Figure 4C), and, to a lesser extent, in the Phe-like and Backscattering measurements (Figures 4E and H, respectively). Another interesting aspect in this figure is the relative agreement between high-oxygen (blue in Figure 4C) and high-Chl-a patches (green in Figure 4D), possibly due to active mixing in the surface layer.

During the return transect (Figure 5), most of the stronger PAHs signals (Naph-like and Phe-like) have disappeared except near ~ 60 km where again a chimney-like feature is associated with higher PAHs, CDOM and Backscattering and lower O_2 concentrations. A thin layer of higher PAH concentrations is visible in the near surface region. It is not clear if this is a hydrocarbon signal or a result of the relatively strong Chl-a signal also observed.

3.4 Triangle pattern

The five transects roughly between $T1$ (0 km) and $T2$ (23 km) are displayed in Figures 6 to 10. Only the first one really started/reached $T1$, the others reached the proximity of Troll B (See track Figure 1). In order to focus on PAHs, Naph-like and Phe-like fluorescence from each transects are plotted together in Figures and , respectively. There is a good agreement between Naph-like and Phe-like observations patterns. Concentrations are relatively low and illustrate the intrinsic variability of surface PAH concentrations in the area.

Worth noting among the 5 transects is the presence of what seems to be sediment resuspension at the very end of Transect 5 (high backscattering in Figure 10H). This pattern is also associated with a low-oxygen layer rising from the seafloor towards the mid water column. Isopycnals near the bottom also exhibit wiggles suggesting that turbulence might be at play.

3.5 Virtual mooring

The glider occupied a virtual mooring position at proximity of Troll B for about 43 hours. Results are presented in Figure 13. Not much to report here at first sight. Naph-like and Phe-like signals are quite similar and relatively decoupled from Chl-a (which is a good news). CDOM signal is also marked when PAHs signals are maximum. This maximum signal occurs after 18 : 00 and is restricted to a thin cold and less saline surface layer.

4 Concluding remarks

While no important spills were detected, the MiniFluo results have shown that coherent patches of water with different concentration were successfully mapped (e.g., Figure 3). These concentrations are low and their origin (natural or due to offshore activities) are uncertain. In the

eventuality of an important spill, it is very likely that the MiniFluo and the glider would be able to detect it. In this case, the best piloting strategy to adopt is still to be determined, and it is likely that more than one glider would be needed to rapidly track the extent of the spill..

Some interesting features were observed, specially during the first cross-channel transect (Figure 4). Chimney-like patterns of higher hydrocarbon fluorescence is observed to emanate from the seafloor and reach the surface (see Section 3.3). Whether these are seeps from the seafloor, sediment resuspension due to strong winds, or other is not clear. These biochemical patterns are however also visible at the same location (e.g. near 20 km) during the return transects (e.g. Figures 5*CEFGH*).

Finally, the *in situ* calibration method has shown some limitations. This procedure was added to the last moment to the cruise plan and was not realized in optimal conditions. First, samples were taken with a Niskin bottle deployed by hand and only 4 samples (with the deepest being only 40 m). For best results, a full depth profiles should have been realized (a possibly replicates). Second, samples were not kept in ideal conditions and were only stabilized one week after collection (temperature was not kept constant during this time). Third, the wrong type of oil was used for preparing the WAF. It is therefore not possible to calibrate the fluorescence directly on these 4 water samples. While Phe-like concentrations derived from fluorescence are in relatively good agreement with the GC-MS measurements, Naph-like concentrations derived from fluorescence are likely overestimated. The presence of Tryptophan in the water column, a compound with he same $\lambda_{\mathrm{Ex}}/\lambda_{\mathrm{Em}}$ couple as the Naphthalene may be responsible for this mismatch.

5 Tables and figures

TABLE 1 – Concentration of total Phenanthrenes and Naphthalenes (methylated and non-methylated) .

Depth (m)	**Naphs** ($\mathrm{ng\,L^{-1}}$)	**Phes** ($\mathrm{ng\,L^{-1}}$)
0	152.4	12.6
10	186.6	1.9
25	137.0	24.0
40	81.1	1.0

TABLE 2 – Glider tracks waypoints. Color code refers to Figure 1.

	Lat (°N)	Lon (°E)	Decimal coordinates
Platforms (magenta & blue stars)			
Troll A	60°39.38'	3°43.62'	[60.6563 ; 3.7270]
Troll B	60°46.51'	3°29.53'	[60.7752 ; 3.4922]
Troll C	60°53.30'	3°36.54'	[60.8883 ; 3.6090]
Songa En.	60°45.150'	3°26.237'	[60.7525 ; 3.4373]
Songa Eq.	60°49.811'	3°34.192'	[60.8302 ; 3.5699]
Cosl Pro.	60°46.041'	3°36.492'	[60.7673 ; 3.6082]
Glider track : T1-L2-L1-T1-T2-T3-T1 is ∼180 km total			
L1	60°45.00'	3°12.00'	[60.7500 ; 3.2000]
L2	60°55.00'	4°20.00'	[60.9167 ; 4.3333]
T1	60°46.80'	3°24.60'	[60.7800 ; 3.4100]
T2	60°40.20'	3°48.00'	[60.6700 ; 3.8000]
T3	60°52.20'	3°33.00'	[60.8700 ; 3.5500]

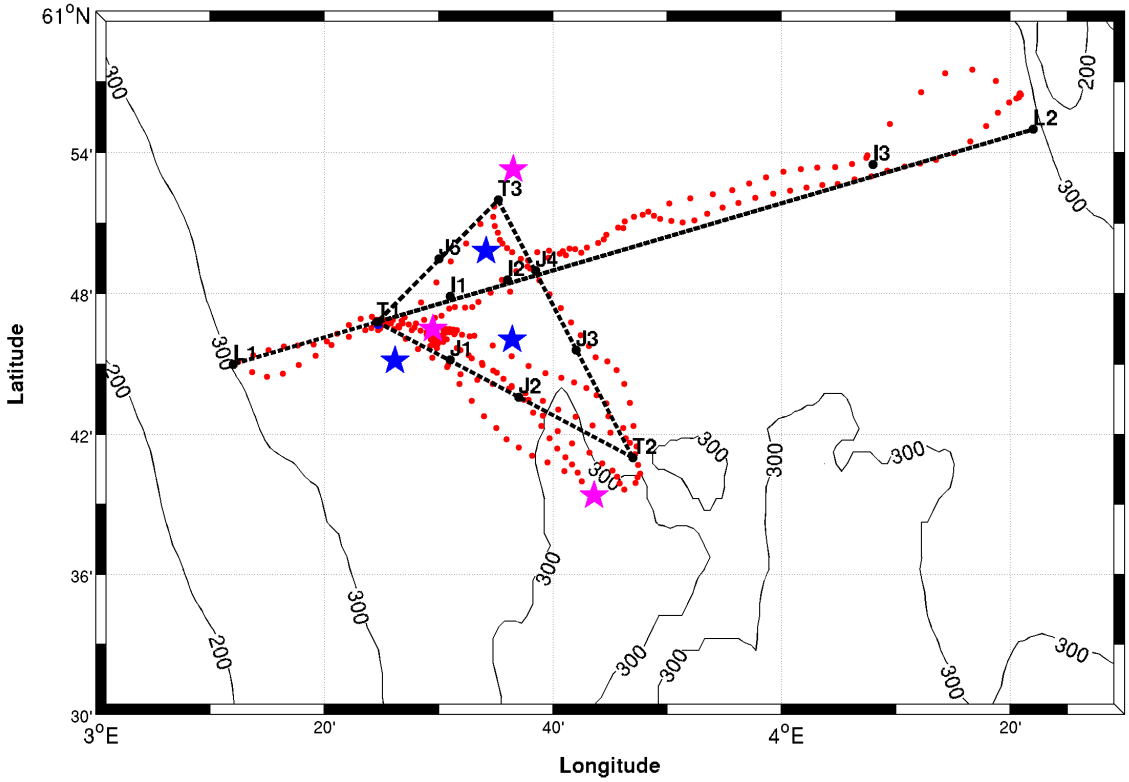

FIGURE 1 – Glider track completed during the deployment in the North Sea. Each red dot correspond to a glider yo (downcast+upcast). Troll platforms A, B and C are shown with magenta stars. Songa Endurance (SEn), Songa Equinox (SEq) and Cosl Promoter (CP) platforms are shown in blue. Black dots and reference letters are waypoints used for piloting.

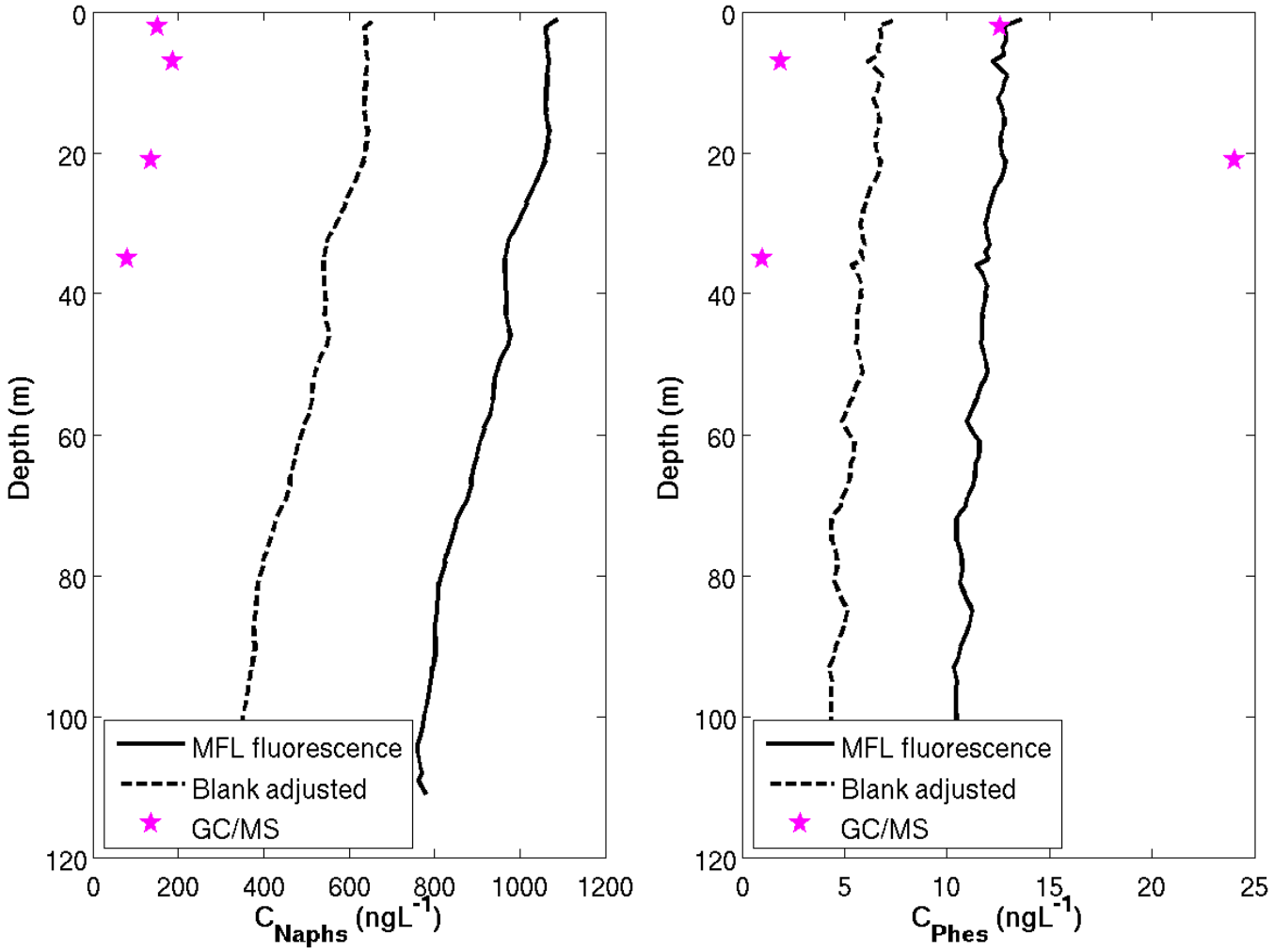

FIGURE 2 – Comparison between PAHs concentrations derived from MiniFluo fluorescence measurements and Gas Chromatography / Mass Spectrometry (GC-MS) analyses performed on water samples. *Left* : Naphthalenes concentrations. *Right* : Phenanthrenes concentrations. Concentration profiles derived from fluorescence using laboratory calibration on water accommodated fraction (WAF) of Maya petroleum are drawn in solid black. The dashed profile represent the profile after the dataset was corrected for environmental blank value (i.e., after subtracting the minimal relative unit value of the dataset.)

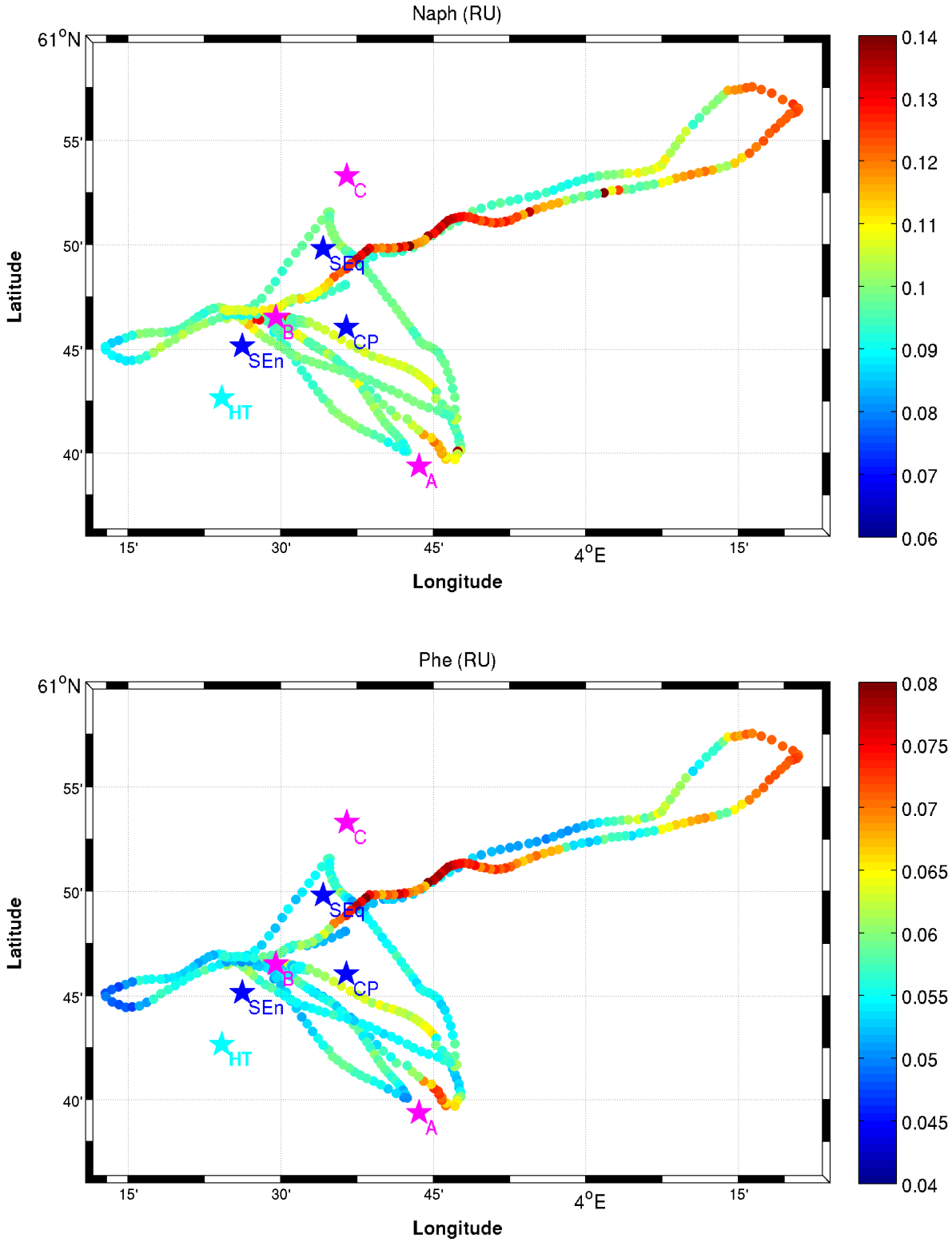

FIGURE 3 – Surface relative-unit (RU) concentrations averaged over the 0-10 m depth range along the glider track. *Upper* : Naphthalene-like fluorescence. *Lower* : Phenanthrene-like fluorescence.

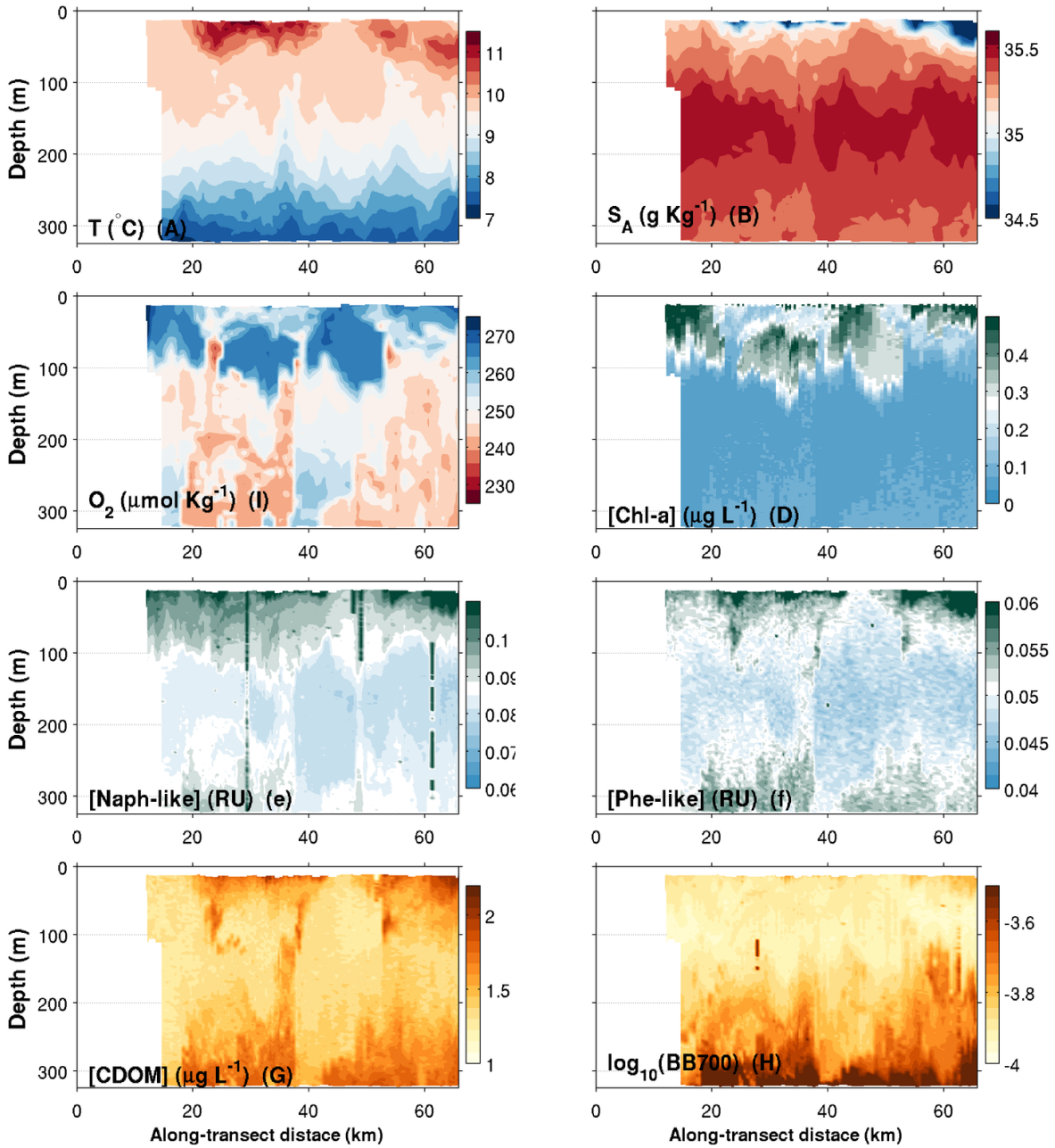

FIGURE 4 – Contours plots of various variables measured by the glider in function of depth and along-transect distance along the line $L1$-$L2$ (see map Figure 1). *a*) Conservative temperature ; *b*) Absolute salinity ; *c*) Dissolved oxygen concentration ; *d*) Chlorophyll-*a* concentration ; *e*) Naphthalene-like concentration ; *f*) Phenanthrene-like concentration ; *g*) Humic-like concentration ; *h*) Turbidity measured as the backscattering signal at 700 nm. Isopycnals are plotted in each panel with thin solid light gray lines (values identified in panels *a* and *b*).

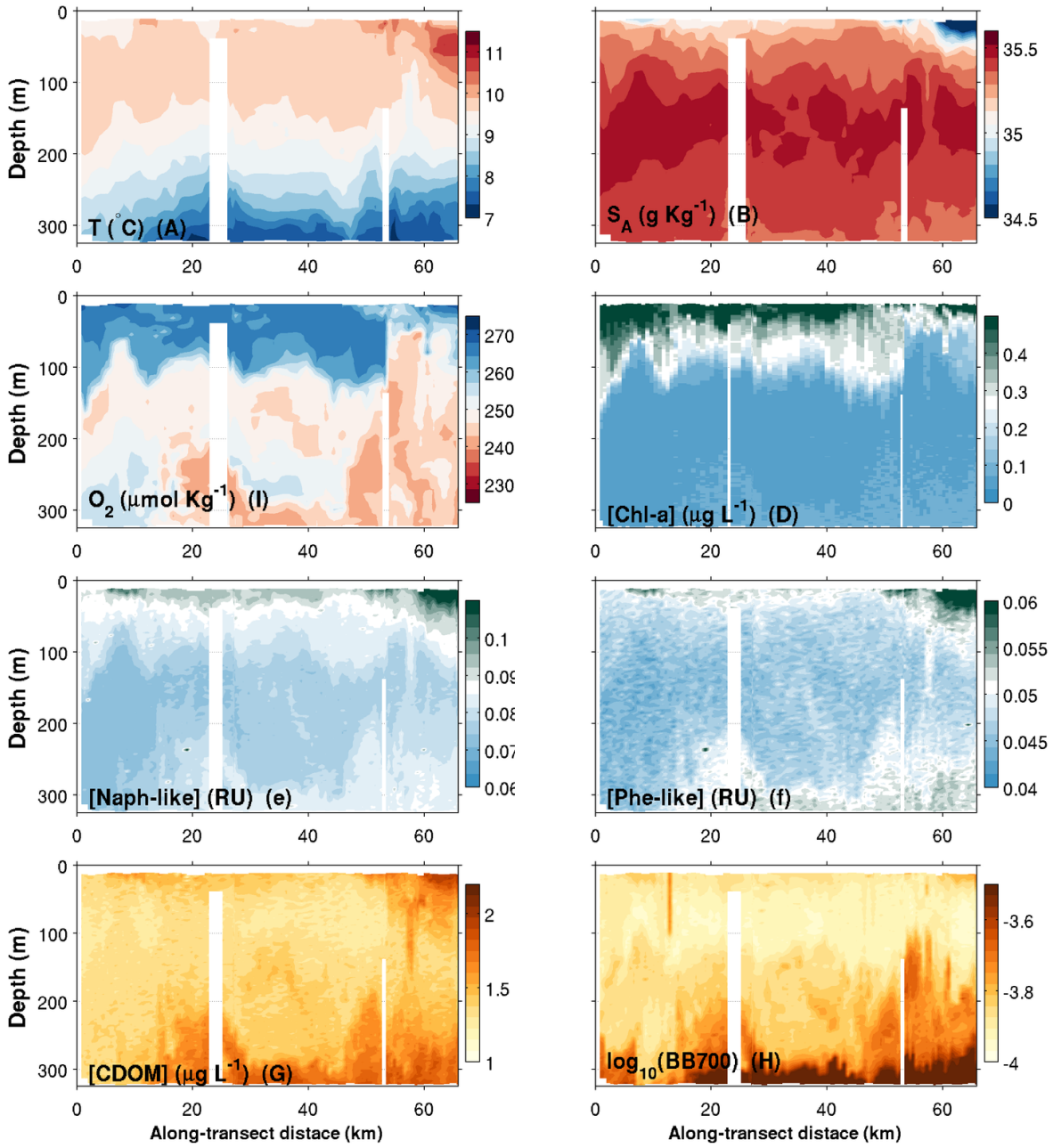

FIGURE 5 – Same as Figure 4, but for the return transect ($L2$-$L1$)

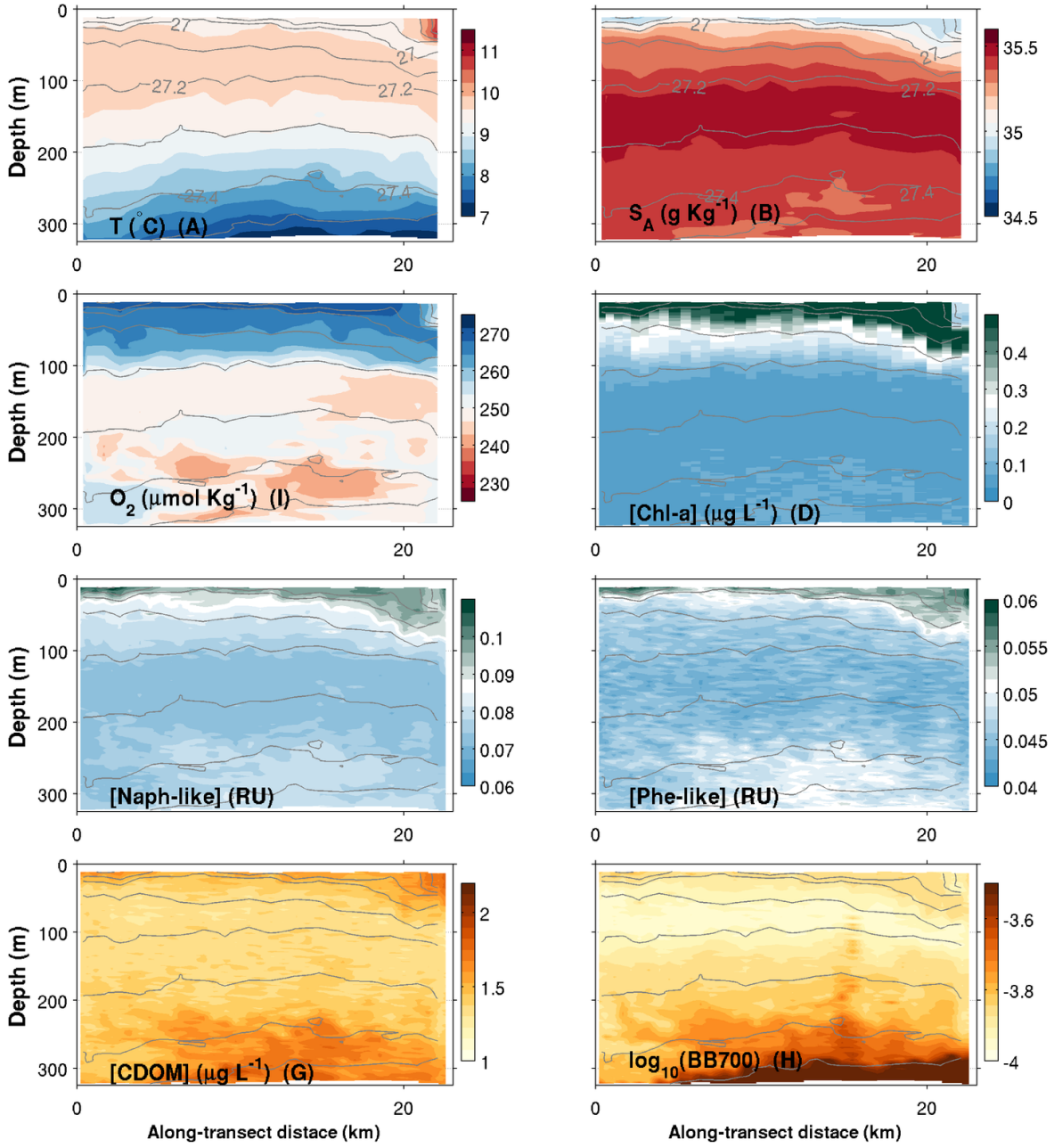

FIGURE 6 – Same as Figure 4, but for the 1st transect along $T1$-$T2$, i.e., one triangle arete (roughly between Troll A and Troll B, see map). The transect was repeated 5 times (Figures 6-10).

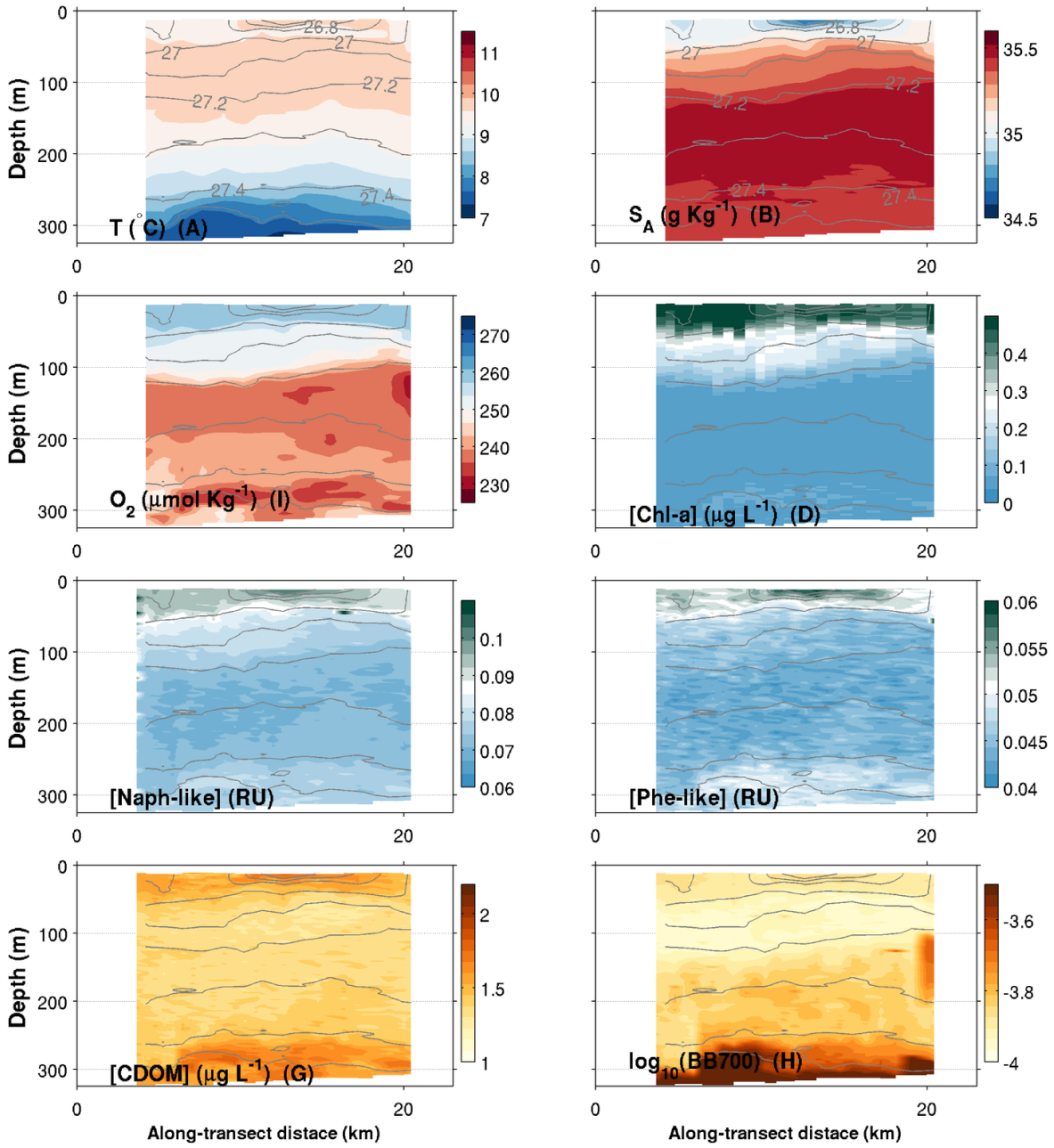

FIGURE 7 – Same as Figure 6, but for the 2nd transect along $T1$-$T2$.

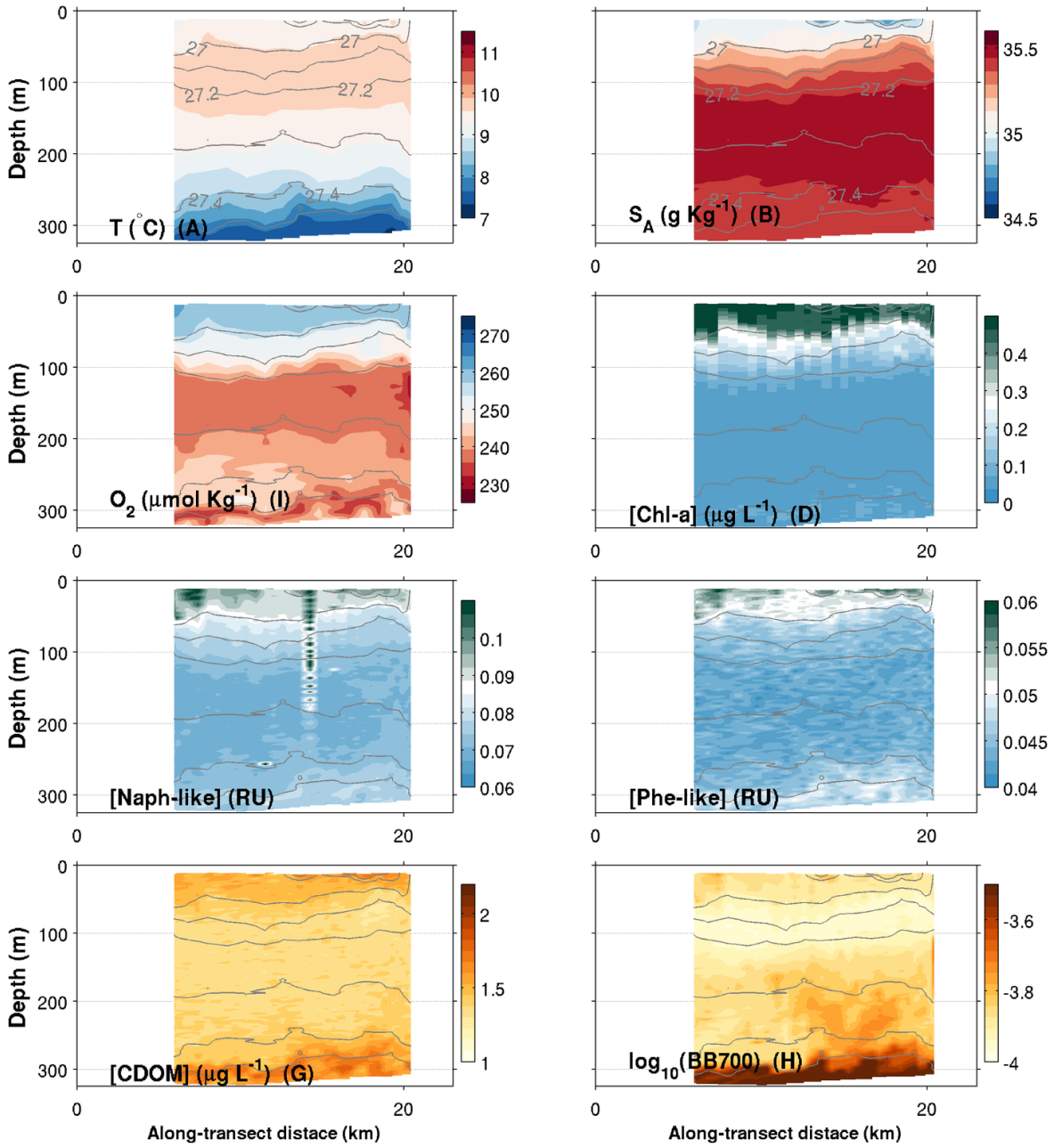

FIGURE 8 – Same as Figure 6, but for the 3rd transect along $T1$-$T2$.

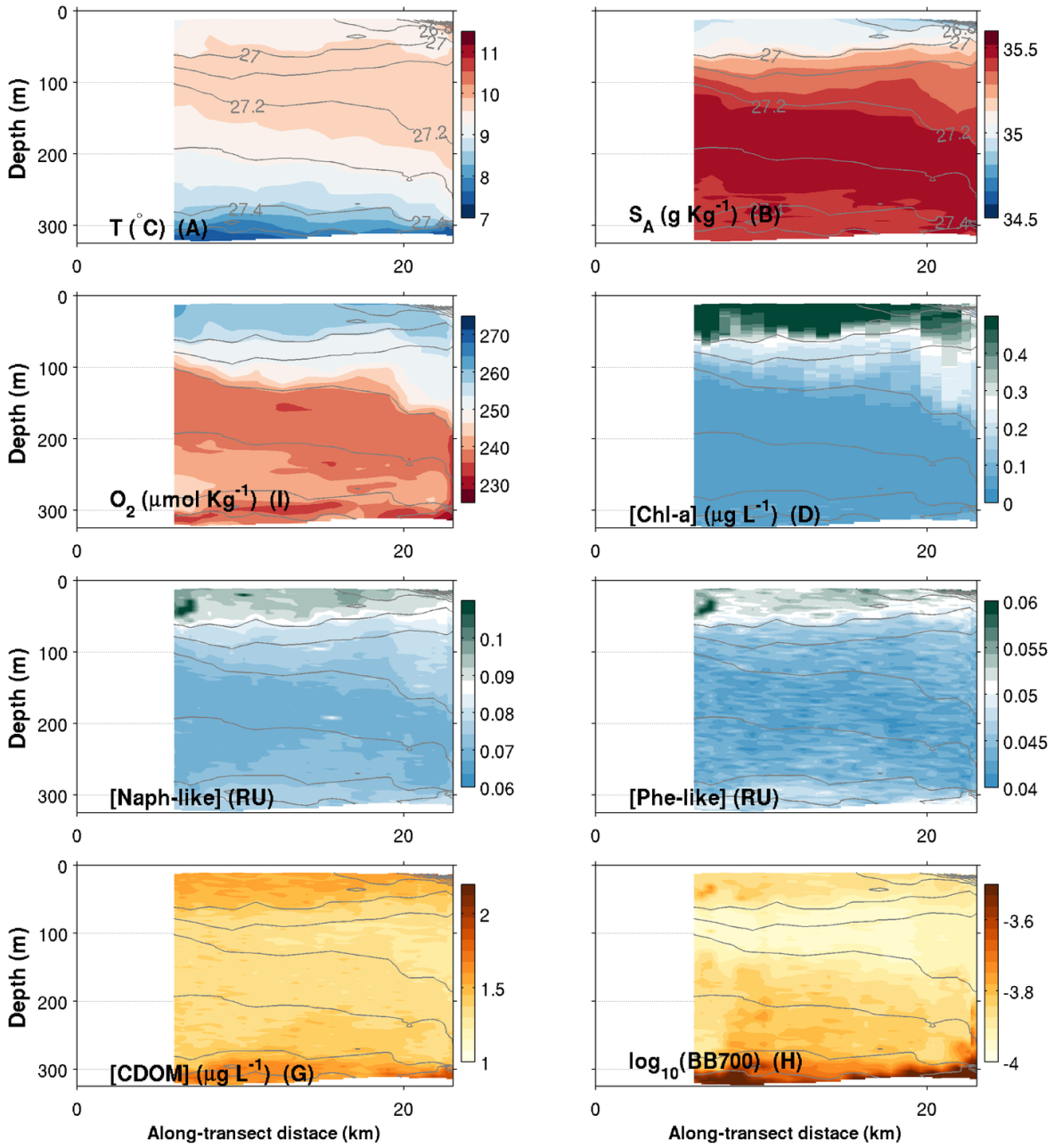

FIGURE 9 – Same as Figure 6, but for the 4th transect along $T1$-$T2$.

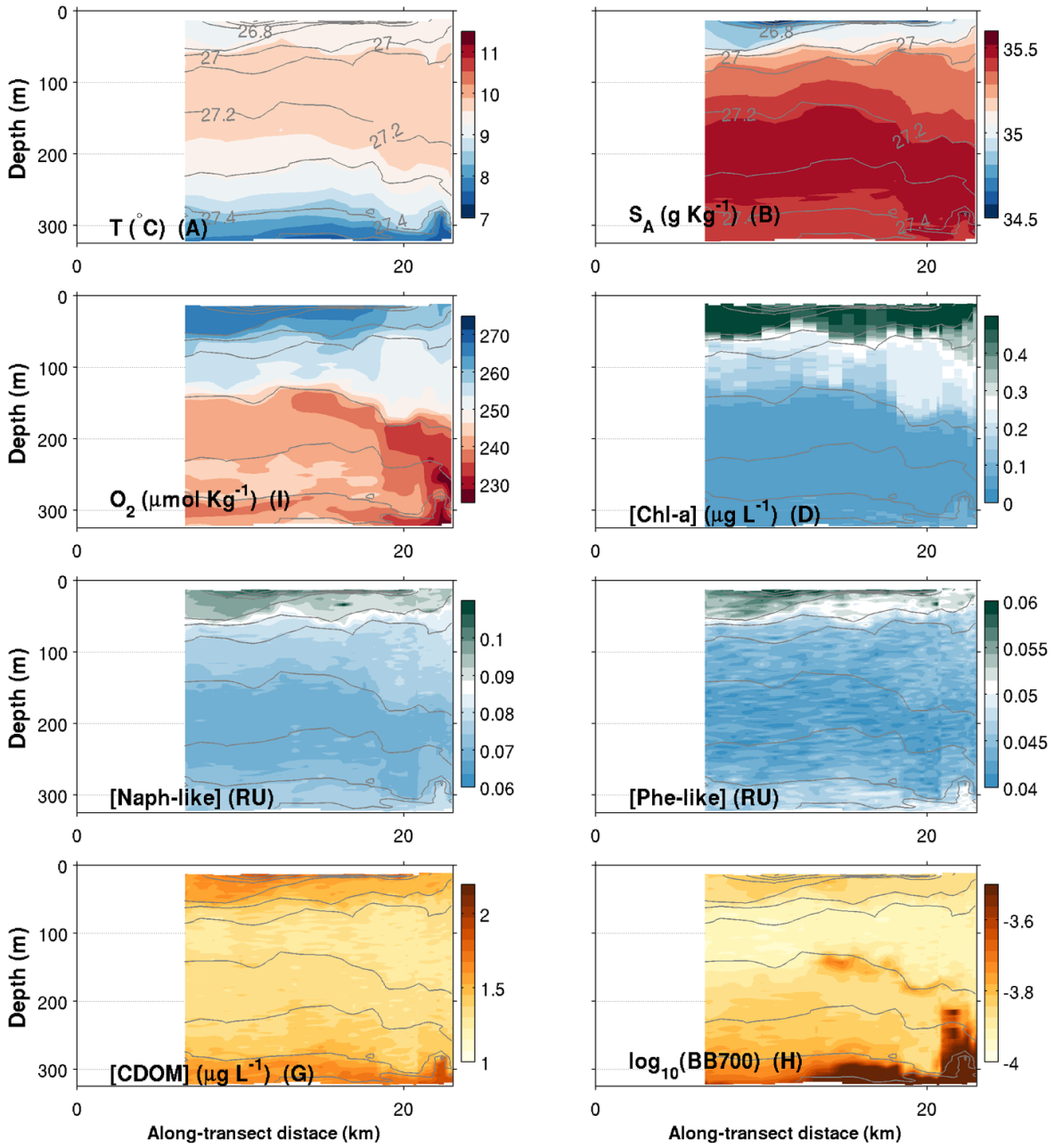

FIGURE 10 – Same as Figure 6, but for the 5th transect along $T1$-$T2$.

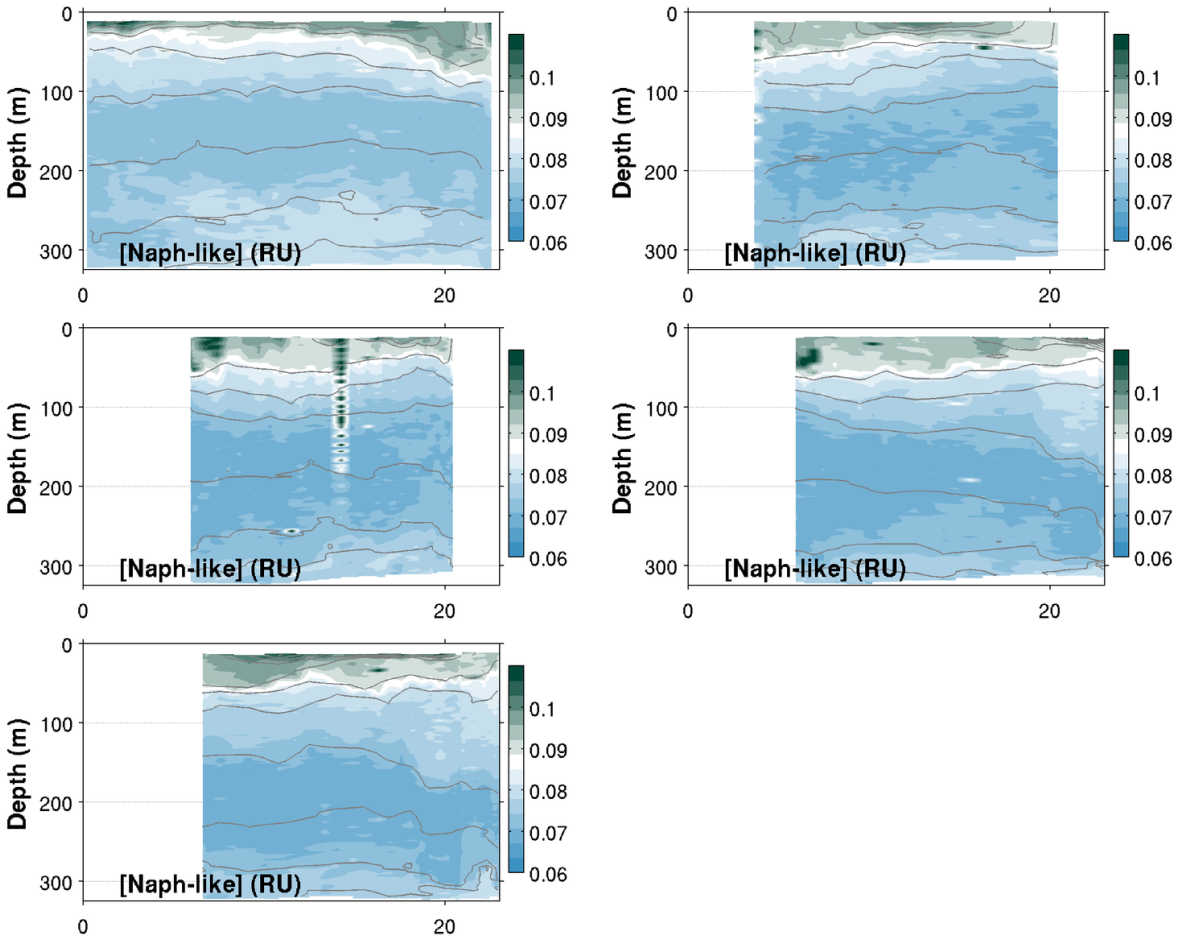

FIGURE 11 – Naph-like fluorescence (relative units) for the 5 transects along $T1$-$T2$.

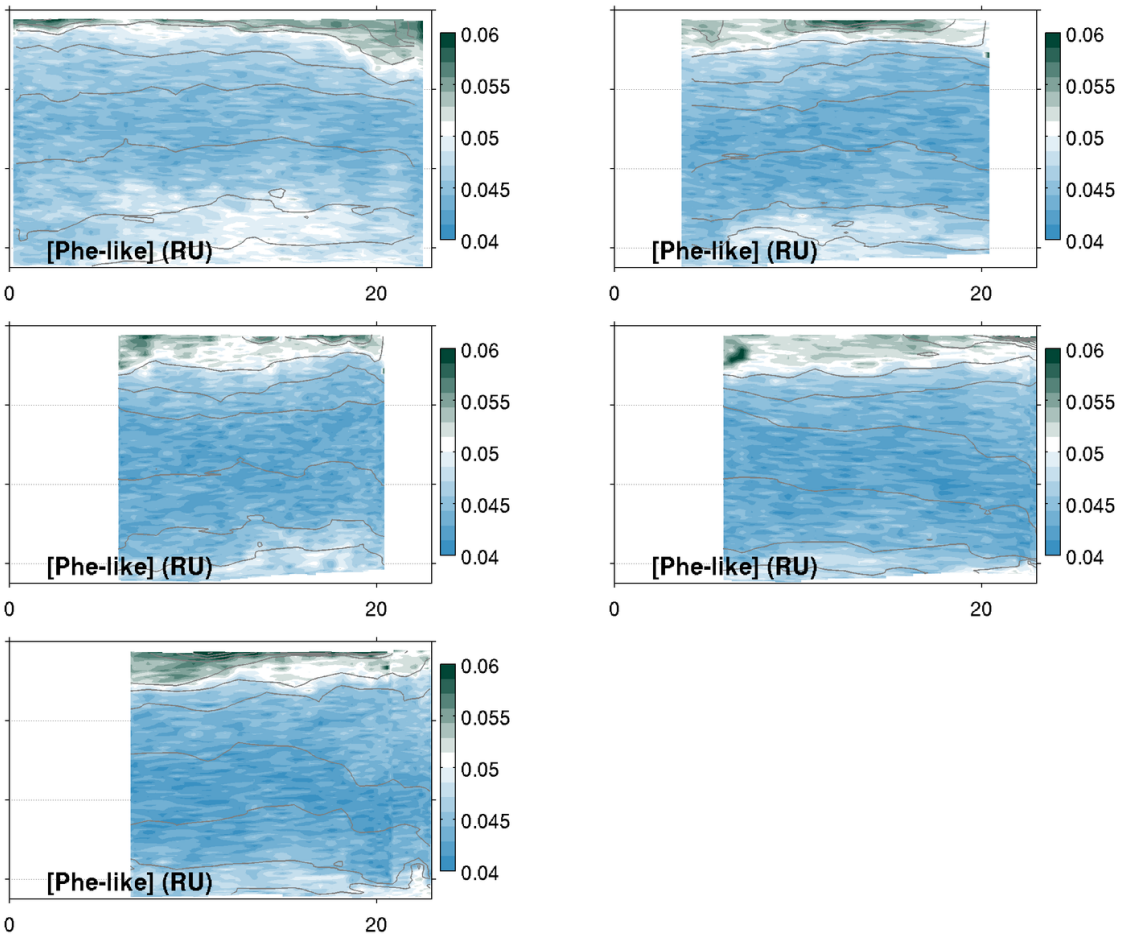

FIGURE 12 – Phe-like fluorescence (relative units) for the 5 transects along $T1$-$T2$.

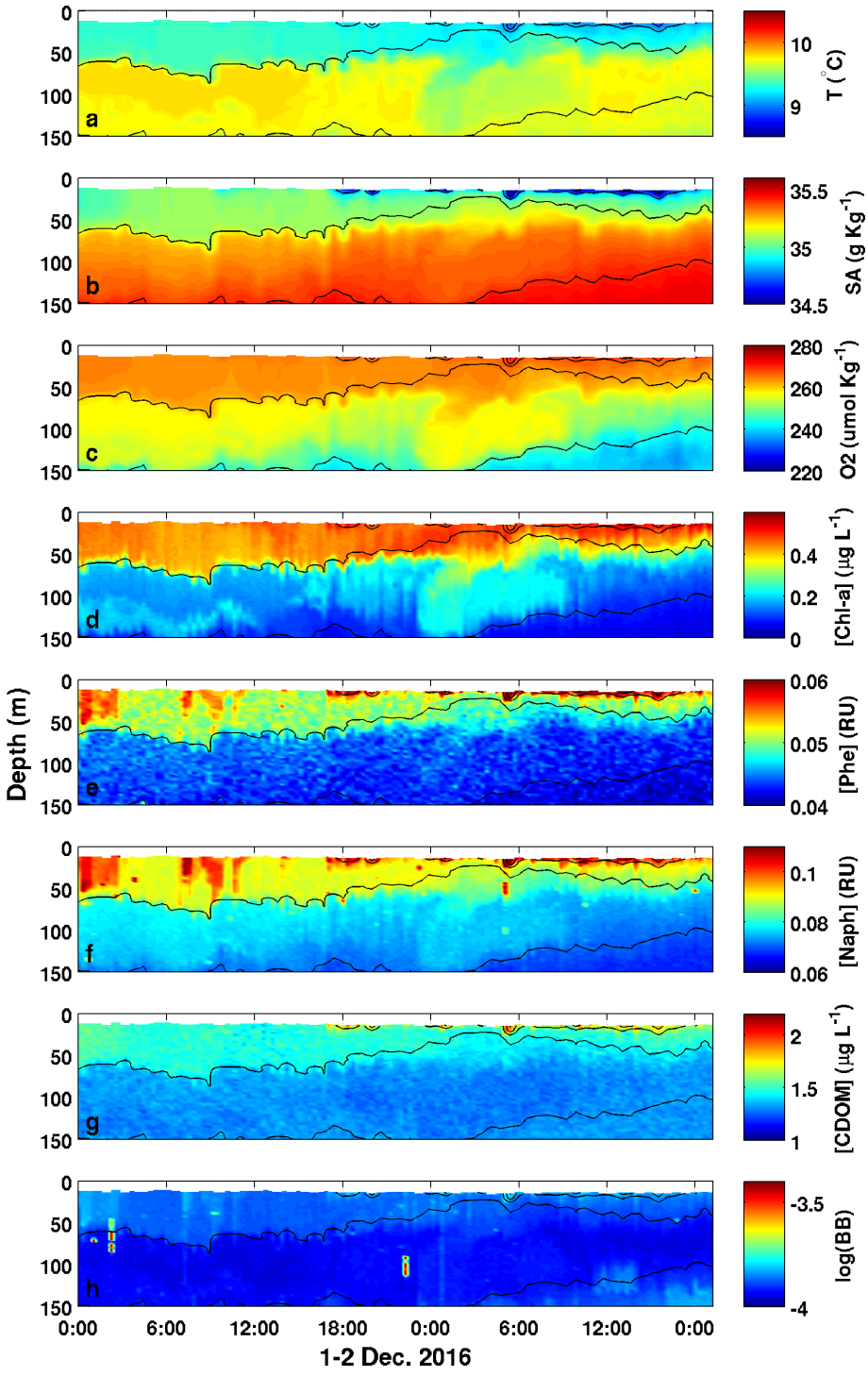

FIGURE 13 – Time-depth contours plots of various variables measured by the glider during the virtual mooring completed at proximity of Troll B near the end of the mission. *a*) Conservative temperature ; *b*) Absolute salinity ; *c*) Dissolved oxygen concentration ; *d*) Chlorophyll-*a* concentration ; *e*) Phenanthrene-like concentration ; *f*) Naphthalene-like concentration ; *g*) Humic-like concentration ; *h*) Turbidity measured as the backscattering signal at 700 nm. Isopycnals are plotted in each panel with thin solid light black lines.

Références

Adhikari, P. L., K. Maiti, and E. B. Overton (2015), Vertical fluxes of polycyclic aromatic hydrocarbons in the northern Gulf of Mexico, *Marine Chemistry*, *168*, 60–68, doi :10.1016/j.marchem.2014.11.001.

Cyr, F., M. Tedetti, F. Besson, L. Beguery, A. M. Doglioli, A. A. Petrenko, and M. Goutx (2017), A new glider-compatible optical sensor for dissolved organic matter measurements : test case from the NW Mediterranean Sea, *Frontiers in Marine Science*, (In Press).

Ferretto, N., M. Tedetti, C. Guigue, S. Mounier, R. Redon, and M. Goutx (2014), Identification and quantification of known polycyclic aromatic hydrocarbons and pesticides in complex mixtures using fluorescence excitation-emission matrices and parallel factor analysis, *Chemosphere*, *107*, 344–353, doi :10.1016/j.chemosphere.2013.12.087.

Guigue, C., M. Tedetti, S. Giorgi, and M. Goutx (2011), Occurrence and distribution of hydrocarbons in the surface microlayer and subsurface water from the urban coastal marine area off Marseilles, Northwestern Mediterranean Sea, *Marine Pollution Bulletin*, *62*(12), 2741–2752, doi :10.1016/j.marpolbul.2011.09.013.

Nasher, E., L. Y. Heng, Z. Zakaria, and S. Surif (2013), Concentrations and sources of Polycyclic Aromatic Hydrocarbons in the seawater around Langkawi Island, Malaysia, *Journal of Chemistry*, *975781*, doi :10.1155/2013/975781.

Wang, Z., M. Fingas, and D. S. Page (1999), Oil spill identification, *Journal of Chromatography A*, *843*(1-2), 369–411, doi :10.1016/S0021-9673(99)00120-X.